

Prediction of Sound Speed in Natural-Gas Mixtures using the CP-PC-SAFT Equation of State

I. V. Prikhod'ko^{a,*}, A. A. Samarov^a, A. M. Toikka^a, and M. Farzaneh-Gord^b

^aSt. Petersburg State University, St. Petersburg, Russia

^bFerdowsi University of Mashhad, Mashhad, Iran

*e-mail: i.prikhodko@spbu.ru

Received June 16, 2020; revised June 23, 2020; accepted June 26, 2020

Abstract—An equation of state based on the perturbed-chain statistical associating fluid theory (PC-SAFT) for estimates of sound speed in natural-gas mixtures is successfully applied in this work. Prediction results of the speed of sound for five binary and six multicomponent systems (dataset includes 1000 data points taken from literature) containing hydrocarbons, nitrogen, and carbon dioxide in a wide range of temperatures (250–415 K) and pressures (0.1–60 MPa) are presented. The fitting parameters of the binary interaction were not used in the calculations. The results of modeling for the speed of sound are shown to be in good agreement with the literature data.

Keywords: thermodynamic properties, equation of state, natural gas, speed of sound, PC-SAFT

DOI: 10.1134/S004057952006010X

INTRODUCTION

The speed of sound is an important thermodynamic quantity extensively used to characterize systems containing oil and gas components and fluids in single- and two- or multiphase states in a broad range of temperatures and pressures [1–5]. Measurements of the thermodynamic properties for fluid mixtures often deal with an estimate of the speed of sound, since the latter helps determine the density; the component composition; and, as a consequence, the molecular weight of the mixture [6–8]. This thermodynamic property is of particular interest from a theoretical viewpoint for those researchers who are testing the capabilities of thermodynamic models, including equations of state (EOS's), for an accurate evaluation of sound speed; this quantity is expressed via the second-order derivative of the Helmholtz energy with respect to volume [9]. The speed of sound (u) is calculated in accordance with well-known equation [10]

$$u = \sqrt{-\frac{V^2 C_p}{M_w C_V} \left(\frac{\partial P}{\partial V} \right)_{T,n}}, \quad (1)$$

where V is the total volume of the system; C_p and C_V are isobaric and isochoric heat capacities, respectively; M_w is the molecular mass of the system, taking into account the number of moles and the molecular masses of all components; and $\left(\frac{\partial P}{\partial V} \right)_{T,n}$ is the derivative of pressure with respect to the total volume at given values of temperature and total number of moles of the

system. Many equations of state (including van der Waals type EOS's) cannot accurately describe the value of the speed of sound [9].

Among the modern equations of state that have been tested in recent years by various researchers to improve the quantitative description of the speed of sound in pure and mixed fluids of various nature, the equations of the SAFT (Statistical Associating Fluid Theory) family stand out. An original EOS based on SAFT has been proposed in [11] and further developed in [12, 13]. One successful modification of this model is perturbed-chain SAFT (PC-SAFT) [14]. This EOS is based on the perturbation theory [15], in which the reference “unperturbed” term of the equation represents a chain of hard spheres to describe the repulsive forces, and the terms associated with the perturbation reflect different interactions taking into account the attractive forces. It is assumed for associating fluids that the surface of a molecule has contact sites which are capable of specific interactions with contact sites of other molecules to mimic hydrogen bonding.

At present, a whole family of equations of state based on PC-SAFT can be talked about; in particular, new versions of this EOS are proposed, and the authors emphasize a more accurate estimate of the speed of sound [10, 16–23], while the description of P - V - T properties, together with the density of a fluid and the saturated vapor pressure, remains reliable. One of the most successful variants of PC-SAFT is critical-point-based PC-SAFT (CP-PC-SAFT). This EOS developed in [16, 17, 20, 23] provided a better

accuracy in describing the speed of sound in various pure fluids and binary systems in a wide range of conditions, including the single- and two-phase states and the near-critical region. The authors overcame some shortcomings of the original version of PC-SAFT (inaccurate estimate of the speed of sound in the liquid phase, overestimated values of the critical constants of pure substances, and incorrect behavior of heat capacities at very high pressures) and introduced insignificant improvements into the expressions for terms in the “residual” Helmholtz energy to refine a description of the thermodynamic properties of pure and mixed fluids. However, the validation of this EOS is still insufficient: it has not yet been rigorously tested for its ability to predict the speed of sound in multi-component systems. Recently, the PC-SAFT family model (CP-PC-SAFT) has been first applied to estimate the speed of sound for a number of multicomponent systems containing oil and gas fluids [24].

The objective of this work is to continue the study we began on applying this equation of state in order to obtain a more complete picture of the estimate of the speed of sound with the aid of CP-PC-SAFT, extending the ability of the model for predicting the speed of sound for binary systems formed by oil and gas components and natural-gas mixtures containing from five to ten components using the standardized critical-point-based approach proposed in [17] in the calculations. To achieve this goal, the task of the work included an estimate of missing model parameters for several pure components.

THEORY

According to the CP-PC-SAFT model, the expression for the “residual” (due to the intermolecular interaction) contribution to the Helmholtz energy (A_{res}) in the system containing nonpolar components can be written as follows (by analogy with the PC-SAFT equation of state):

$$A_{res} = A^{hs} + A^{chain} + A^{disp} = A^{hc} + A^{disp}, \quad (2)$$

where the first term in the latter sum (A^{hc}) is connected with the contribution from the formation of chains (A^{chain}) from hard spheres (A^{hs}), and the second is connected with the dispersion contribution of the Helmholtz energy responsible for the attraction-related interactions (A^{disp}). The formulas for calculating the addends in (2) have been reported elsewhere [14, 17, 20], including useful expressions for thermodynamic properties related with first- and second-order derivatives of the Helmholtz energy with respect to volume (density). An expression for the EOS, written in terms of the compressibility factor or pressure, can be easily derived from (2) with the aid of the known formulas of thermodynamics.

Here, the main refinements to the CP-PC-SAFT EOS proposed in [17] in comparison with the original PC-SAFT are presented. To avoid the prediction of the negative heat capacities and the isotherms intersections at extremely high pressures (which has no physical meaning and was observed in the PC-SAFT modeling), the expression of the hard sphere contribution (A^{hs}) has been modified. The corresponding refined expression for the residual contribution to the Helmholtz energy is as follows:

$$A^{hs} = RT \frac{m}{\xi_0} \left(\frac{3\xi_1\xi_2}{1-\xi_3} \right) + \frac{\xi_2^3}{\xi_3(1-\xi_3)^2} + \left(\frac{\xi_2^3}{\xi_3^2} - \xi_0 \right) \ln \left[1 - \xi_3 \sqrt{\frac{d^3(\xi_3-1)}{\xi_3\sigma^3 - d^3}} \right], \quad (3)$$

where m is the number of segments, σ is the segment diameter, ε/k is the segment energy parameter divided by Boltzmann's constant, $d = \sigma\theta$, and the dimensionless quantity θ is given by the expression

$$\theta = \frac{1 + 0.2977(k/\varepsilon)T}{1 + 0.33163(k/\varepsilon)T + 0.0010477(k/\varepsilon)^2 T^2}. \quad (4)$$

This factor, taking into account the temperature dependence of the segment diameter, has been introduced to obtain a correct description at the infinity temperature limit and reasonably predict the inversion curve of the Joule–Thomson effect. Additionally,

$$\zeta_k = \frac{\pi N_{av}}{6v} \sum_i x_i m_{ii} d_{ii}^k, \quad (5)$$

$$A^{chain} = RT \sum_{i,j} x_i x_j (1 - m_{ij}) \ln \left[g_{ij}(d_{ij})^{hs} \right], \quad (6)$$

where the segment radial distribution function is written as

$$g_{ij}(d_{ij})^{hs} = \frac{1}{1-\xi_3} + \frac{3d_{ii}d_{jj}\xi_2}{(d_{ii}+d_{jj})(1-\xi_3)^2} + 2 \left(\frac{d_{ii}d_{jj}}{d_{ii}+d_{jj}} \right)^2 \frac{\xi_2^2}{(1-\xi_3)^3}. \quad (7)$$

The dispersion term expression of the Helmholtz energy contains the analytical functions (I_1 and I_2), which represent the integrals of the radial distribution function in the first- and second-order perturbation terms:

$$A^{disp} - RN_{av} \left(\frac{2\pi(\epsilon/k)m^2\sigma^3}{v} \right) I_1 + \frac{\pi(\epsilon/k)^2 m^3 \sigma^3}{vT(1+m(8\zeta_3-2\zeta_3^2)/(1-\zeta_3)^4 + (1-m)(20\zeta_3-27\zeta_3^2+12\zeta_3^3-2\zeta_3^4)/((1-\zeta_3)(2-\zeta_3))^2)} I_2, \quad (8)$$

where

$$I_1 = \sum_{i=1}^6 \left(a_{0i} + \frac{m-1}{m} a_{1i} + \frac{m-1}{m} \frac{m-2}{m} a_{2i} \right) \zeta_{3i}^i, \quad (9)$$

$$I_2 = \sum_{i=1}^6 \left(b_{0i} + \frac{m-1}{m} b_{1i} + \frac{m-1}{m} \frac{m-2}{m} b_{2i} \right) \zeta_{3i}^i. \quad (10)$$

In expressions (9) and (10), a_{0-2i} and b_{0-2i} are the universal model parameters whose values can be found elsewhere [17]; universal parameters of the radial distribution function in the first-order perturbation term have been refitted using the second and third virial coefficients of n -alkanes. When the EOS is used for mixtures, the mixing rules are applied, introducing adjustable binary interaction parameters k_{ij} for correcting the dispersive interactions term and/or l_{ij} , which take into account differences in the sizes of the segment diameters. More flexible additional mixing rules in the CP-PC-SAFT model in comparison with the original PC-SAFT are proposed:

$$\frac{\epsilon}{k} = \frac{\sum_i \sum_j x_i x_j m_{ii} m_{jj} \sigma_{ij}^3 (\epsilon/k)_{ij}}{\sigma^3 \left(\sum_i x_i m_{ii} \right)^2}. \quad (11)$$

$$\sigma = \sqrt[3]{\frac{\sum_i \sum_j x_i x_j m_{ii} m_{jj} \sigma_{ij}^3}{\left(\sum_i x_i m_{ii} \right)^2}}, \quad (12)$$

$$m = \sum_i x_i m_i, \quad (13)$$

where

$$\sigma_{ij} = \frac{\sigma_{ii} + \sigma_{jj}}{2}, \quad (14)$$

$$m_{ij} = (1 - l_{ij}) \frac{m_{ii} + m_{jj}}{2}, \quad (15)$$

$$(\epsilon/k) = (1 - k_{ij}) \sqrt{(\epsilon/k)_{ii} (\epsilon/k)_{jj}}. \quad (16)$$

In the above formulas, the indices i and j are referred to different segments of the system.

Four parameters for describing a pure nonpolar substance i in terms of the CP-PC-SAFT model are required: the number of segments forming a chain-molecule m_i , the segment diameter σ_i , and the interaction energy parameter divided by Boltzmann's con-

stant for segments of i th type ϵ_i/k , as well as the parameter δv_c responsible for the shift in the critical volume (the ratio between the critical volume calculated by the model to its experimental value). The parameters of the CP-PC-SAFT model for many pure components have been determined [17]; the list of parameters is extending and includes polar and associating components as well [16, 20, 23]. The predictive capability of CP-PC-SAFT is enhanced by a substantial reduction of the data required for evaluating its substance-specific molecular parameters. To find the parameters of the model instead of fitting them using an optimization procedure for processing a large experimental dataset (as is done for the PC-SAFT model), these parameters are determined for two reference points (states), namely, the critical and triple points, by implementing a standardized numerical procedure using the Mathematica package.

CALCULATION METHODOLOGY

A calculation procedure based on the numerical solution of a system of four equations for finding the parameters of the CP-PC-SAFT equation of state is described in detail in [17]. The system of equations has the following form:

$$\left(\frac{\partial P}{\partial V} \right)_{T_c} = 0 \Big|_{V_{c,EOS=\delta v_c}}, \quad (17)$$

$$\left(\frac{\partial^2 P}{\partial V^2} \right)_{T_c} = 0 \Big|_{V_{c,EOS=\delta v_c}}, \quad (18)$$

$$P_{c,EOS} = P_c, \quad (19)$$

$$\rho_{EOS}^L = \rho_{exp}^L \Big|_{\text{в тройной точке}}. \quad (20)$$

The idea of the approach used is that the parameters of the CP-PC-SAFT equation are determined at experimental critical points of pure components (for given values of critical constants) and the liquid density data at a triple point (from thermodynamic databases, for example, NIST [24]). For solving equations (17)–(19), the critical pressure calculated by EOS ($P_{c,EOS}$) is defined by replacing the temperature (T) by critical temperature (T_c) and volume (V) by the EOS's critical volume (V_c , EOS equal to $V_c \delta$). Thereafter, the conditions of the pure component critical point (Eq. (17)–(18)) can be derived analytically. Although in Eq. (20) the experimental value of the density is equated to its value calculated from the EOS, in fact

Table 1. Values of CP-PC-SAFT parameters for pure components used in this study

Component	m	ϵ/k , K	σ , Å	δ	Reference
N ₂	0.99880	94.351	3.61590	1.10537	[17]
CO ₂	2.03351	163.491	2.81786	1.17358	[17]
CH ₄	1.00082	142.508	3.74760	1.12673	[17]
C ₂ H ₆	1.56358	185.392	3.57406	1.16657	[17]
C ₃ H ₈	2.41440	184.368	3.39176	1.15188	[17]
<i>n</i> -C ₄ H ₁₀	2.48262	209.446	3.65040	1.15976	[17]
<i>i</i> -C ₄ H ₁₀	2.16530	213.128	3.84220	1.15340	This work
<i>n</i> -C ₅ H ₁₂	3.06424	212.528	3.62421	1.16385	[17]
<i>i</i> -C ₅ H ₁₂	3.06420	212.528	3.62420	1.15640	This work
<i>n</i> -C ₆ H ₁₄	3.51081	218.238	3.65575	1.16091	[17]

the actual solution is reduced to the equality of pressures at the triple point (P_{tp} EOS = P_{tp}). This is due to the fact that the equation of state is expressed in terms of pressure as a function of temperature and density. At the same time, if the temperatures (the densities) are identical, the pressures must be equal as well. System of equations (17)–(20) can be solved analytically; however this procedure is tedious and yields different sets of solutions, which requires the further creation of final solutions for selecting the algorithm. Unlike that, the numerical procedure yields only one set of solutions; it is necessary to specify the initial estimations for model parameters.

Most of the CP-PC-SAFT parameters for typical oil and gas components have been obtained and published in [17]. In the present work, the values of

unavailable parameters for two isoalkanes—*isobutane* and *isopentane*—were estimated. All values of parameters used for pure substances are listed in Table 1.

Good results of describing thermodynamic properties for various pure fluids—light hydrocarbons (methane, ethane, and propane), heavier alkanes, carbon dioxide, nitrogen, and some binary and ternary systems composed of natural-gas components—have been previously obtained [17]. To check the predictive ability of the EOS in calculating the speed of sound for binary subsystems and multicomponent mixtures, the binary interaction parameters (l_{ij} and k_{ij} in equations (15), (16)) were not adjusted and were set to be zero. It should be noted that the PC-SAFT model itself makes it possible to predict thermodynamic properties and phase behavior for multicomponent systems using only the parameters of pure components. At the current stage of our research, an alternative approach requiring additional fitting parameters has not been considered.

RESULTS AND DISCUSSION

First, we tested the capability of the CP-PC-SAFT to predict the speed of sound in pure methane as a main substance of the natural-gas mixtures under consideration. As was depicted in Fig. 1, no large deviations were observed between the values measured experimentally [25] and those predicted from the model. It is worth noting that the CP-PC-SAFT is competitive with other PC-SAFT-based models in describing the speed of sound in methane [10, 17, 19, 21, 22]. Modeling pure components is an important test for any EOS; however, the main practical intention for the EOS is to predict thermodynamic properties for mixtures. In this regard, the asymmetric natural-gas mixtures formed by various hydrocarbons and nonhydrocarbons is of special interest.

Further, we used the CP-PC-SAFT in estimating the speed of sound for binary and multicomponent

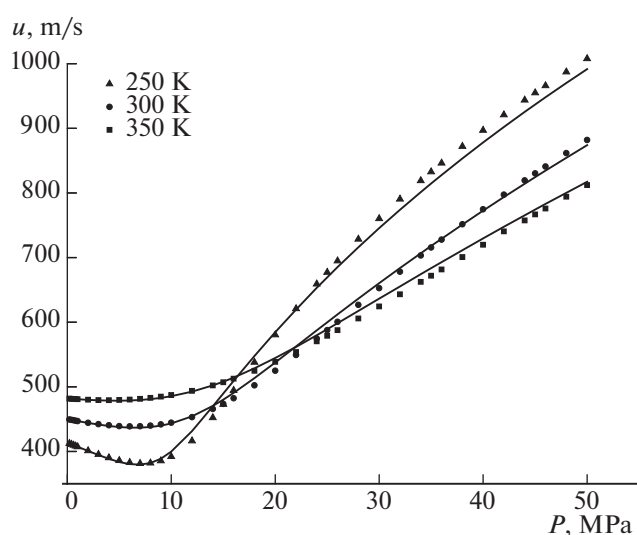


Fig. 1. Dependence of the speed of sound in methane on pressure. Points are experimental values [25] and lines are prediction results using CP-PC-SAFT.

mixtures formed by components of natural gas with various methane contents. The limited experimental information for the speed of sound in multicomponent systems used in this study is not crucial for evaluating the predictive abilities of the model. Not many experimental datasets taken from the literature were treated, but they were sufficient for modeling to reflect basic trends in the sound-speed behavior with changes in temperature, pressure, and methane composition. The experimental compositions of binaries and those of multicomponent synthetic/natural-gas mixtures from different fields and corresponding values of the speed of sound in a wide range of pressures for a number of temperatures are given in [26–28].

A comparison of the results given by the CP-PC-SAFT model and experimental data was estimated using mean absolute percentage error (MAPE) values and is given for binary and multicomponent systems in Tables 2 and 3, respectively:

$$MAPE = \frac{100\%}{N} \sum_{i=1}^N \left| \frac{u_i^{pacu}}{u_i^{эксп}} - 1 \right|, \quad (21)$$

where u is the speed of sound, u_i^{pacu} is the value of the speed of sound calculated from the equation of state for i th point, $u_i^{эксп}$ is the experimental value of the speed of sound for the i th point, and N is the number of experimental points.

Prediction results for the speed of sound for binary and multicomponent systems containing natural-gas components together with experimental data are illustrated in Fig. 2.

The results show that the model correctly reflects a slight minimum in the dependence sound speed on pressure at fixed temperature. As can be seen from Fig. 2, the calculations yield good results sufficient for reasonable estimates the speed of sound in the systems examined at the conditions under consideration. A slightly larger discrepancy between experimental and calculated sound speed values is observed for the binary mixtures at the lowest temperatures of 250 and 275 K and pressures within a range 9–10.5 MPa (Figs. 2a–2c, Table 2). At these conditions the sound speed starts to change its direction significantly with an increase in pressure and the predicted curve is a bit

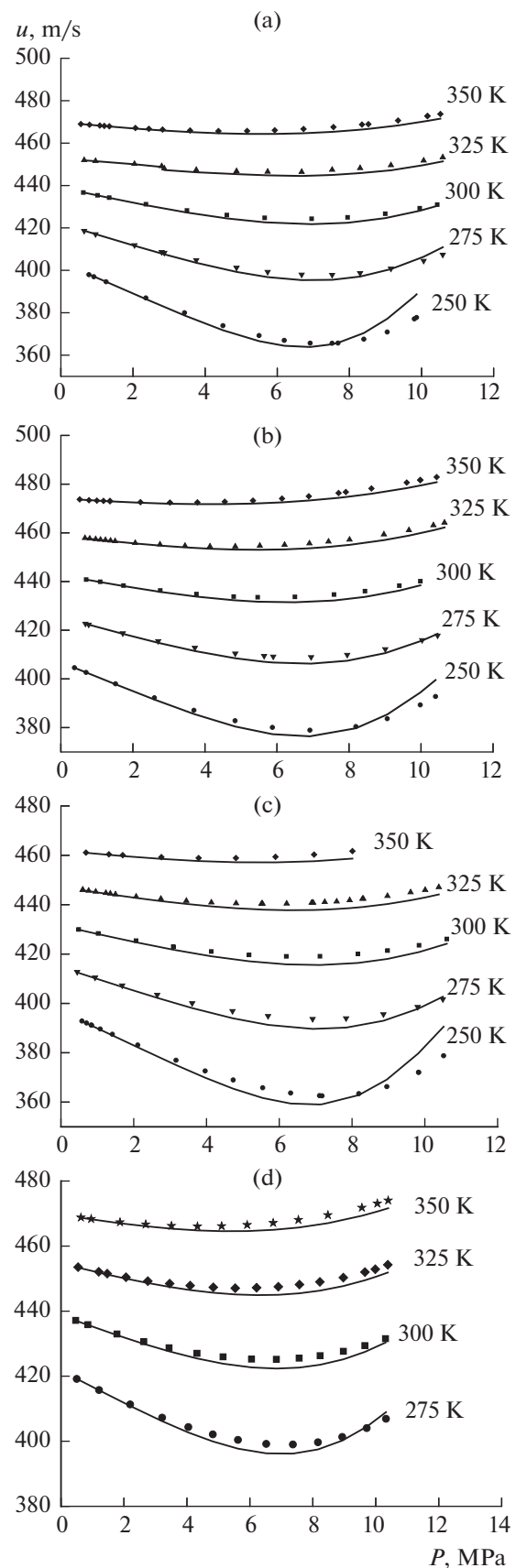


Fig. 2. Dependence of the speed of sound on pressure: (a) points are experimental values for the binary system methane (0.95) + ethane (0.05) [27] and lines are prediction results using CP-PC-SAFT, (b) points are experimental values for the binary system methane (0.95) + nitrogen (0.05) [27] and lines are prediction results using CP-PC-SAFT, (c) points are experimental values for the binary system methane (0.95) + carbon dioxide (0.05) [27] and lines are prediction results using CP-PC-SAFT, and (d) points are experimental values for the natural-gas mixture of Gulf Coast field methane (0.95) + other components (0.05) [27] and lines are prediction results using CP-PC-SAFT.

Table 2. Results obtained in calculations of the speed of sound for the binary mixtures under consideration using CP-PC-SAFT

System	Composition, mol. fraction of the first component	Number of experimental points	Temperature, K	Pressure range, MPa	MAPE for speed of sound, %	Reference
CH ₄ + C ₂ H ₆	0.94985	15	250.00	0.78–9.86	0.75	[27]
		14	275.00	0.65–10.59	0.35	
		12	300.00	0.62–10.44	0.28	
		20	325.00	0.50–10.40	0.23	
		20	350.00	0.55–10.52	0.26	
	0.84902	8	250.00	2.52–19.96	2.37	[28]
		9	275.00	0.52–20.08	1.84	
		9	300.00	0.51–19.75	1.42	
	0.68526	9	350.00	0.55–20.05	0.63	[27]
		11	275.00	0.63–8.47	0.65	
		14	300.00	0.94–10.67	0.75	
		17	325.00	0.69–10.62	0.48	
	0.34524	14	350.00	0.35–10.68	0.45	[27]
		7	250.00	0.25–1.42	0.45	
		10	275.00	0.54–4.21	0.29	
		15	300.00	0.50–6.45	0.46	
17		325.00	0.70–10.37	1.34		
CH ₄ + C ₃ H ₈	0.90016	15	350.00	0.48–10.57	0.75	[27]
		7	250.00	0.48–3.05	0.21	
		11	275.00	0.58–10.22	0.93	
		14	300.00	0.55–10.45	0.44	
		25	325.00	0.48–10.41	0.43	
CH ₄ + N ₂	0.95114	14	350.00	0.62–10.25	0.46	[27]
		29	250.00	0.28–10.40	0.52	
		12	275.00	0.68–10.46	0.31	
		12	300.00	0.70–9.98	0.30	
		21	325.00	0.67–10.65	0.24	
	0.71373	20	350.00	0.52–10.43	0.23	[27]
		17	250.00	0.09–10.07	0.38	
		17	275.00	0.35–9.92	0.45	
		18	300.00	0.10–10.26	0.27	
		29	325.00	0.55–10.01	0.26	
CH ₄ + CO ₂	0.94979	14	350.00	0.93–10.47	0.34	[27]
		19	250.00	0.58–10.52	0.80	
		12	275.00	0.45–10.50	0.48	
		12	300.00	0.49–10.60	0.50	
		28	325.00	0.60–10.38	0.44	
	0.69944	9	350.00	0.69–8.01	0.30	[27]
		16	250.00	0.63–7.48	0.97	
		17	275.00	0.56–10.40	1.20	
		17	300.00	0.69–10.38	1.20	
		20	325.00	0.58–10.45	0.99	
N ₂ + CO ₂	0.49593	15	350.00	0.63–10.37	1.02	[27]
		9	250.00	0.84–3.96	0.30	
		9	275.00	2.04–10.21	0.64	
		11	300.00	1.33–10.03	0.69	
		19	325.00	0.52–10.02	0.63	
		17	350.00	1.75–10.34	0.86	

Table 3. Results obtained in calculations of the speed of sound in the multicomponent systems under consideration using CP-PC-SAFT

Gas mixture or field	Number of experimental points	Temperature, K	Pressure range, MPa	MAPE for speed of sound, %	Reference
Synthetic gas mixture	22	323.31	4.86–56.69	1.14	[26]
	22	346.48	5.11–56.69	1.11	
	24	369.41	4.79–56.90	1.12	
	18	392.34	6.12–56.86	1.27	
	18	415.45	6.90–58.37	1.36	
Gulf Coast	12	250.00	0.59–10.41	0.95	[27]
	13	275.00	0.50–10.33	0.38	
	14	300.00	0.47–10.31	0.38	
	17	325.00	0.54–10.38	0.36	
	14	350.00	0.63–10.40	0.32	
Amarillo	11	250.00	0.67–10.88	1.20	[27]
	10	275.00	0.65–10.47	0.43	
	6	298.00	6.89–23.39	1.71	
	11	300.00	0.56–10.43	0.38	
	19	325.00	0.69–10.43	0.37	
	15	350.00	0.86–10.64	0.30	
Statoil Dry Gas	15	250.00	0.80–9.74	1.52	[27]
	11	275.00	0.52–10.42	0.65	
	18	300.00	0.53–10.30	0.41	
	17	325.00	0.47–10.40	0.42	
Statoil Statvordgass	12	300.00	1.86–10.38	1.37	[27]
	14	325.00	0.42–9.89	0.79	
	16	350.00	0.64–10.44	0.86	
Natural-gas mixture	9	250.00	0.52–19.59	2.50	[28]
	8	275.00	0.52–19.06	1.61	
	9	300.00	0.50–20.06	1.22	
	9	350.00	0.51–20.17	0.53	

steeper in comparison with experimental one. In this case, tuning parameter k_{ij} to improve the predicted results was not necessary due to the generally robust estimates for the speed of sound using CP-PC-SAFT obtained for the two- and multicomponent systems (Fig. 2d, Table 3), which were studied at 250 K and higher temperatures.

The results represented in Figs. 1 and 2a–2c demonstrate that, in accord with the experimental data, the addition of the second component to pure methane leads to a decrease in the speed of sound value for the binary system compared with that for a pure component at a fixed temperature and pressure. Figures 2a–2c show the influence of adding the second component on sound speed (approximately 95 mol. % methane and 5 mol. % of another component, respectively). Taking into account the nonpolar nature

of the mixture components (polarity close to zero), the differences in the sound-speed values for the presented binary subsystems with methane can be associated with the differences in the molecular size of the fluids (two components). The model correctly reproduces the observed dependences.

It can be seen from Table 3 that the MAPE values for the speed of sound do not exceed 2.5% for the multicomponent systems studied, which indicates a rather good accuracy of the results. It is worth noting, as we have shown earlier [24] that, in addition to the speed of sound, CP-PC-SAFT gives fairly accurate results in predicting density for multicomponent mixtures.

An analysis of the contribution from individual terms in Eq. 2 with nonpolar fluid *n*-hexane as an example using PC-SAFT showed [10] that the accurate representation of the second-order derivative of

the Helmholtz energy with respect to volume results in a good estimate of the quantity $\left(\frac{\partial P}{\partial V}\right)_{T,n}$, which, in turn, leads to an accurate speed of sound predictions. Since this derivative is determined by the contribution of hard spheres in the expression for A^{hs} , it can be concluded that a quantitative description of the interactions connected with repulsion would possibly improve the estimate of the partial derivative of pressure with respect to volume and related thermodynamic properties. This is essentially what was achieved in [17] with the CP-PC-SAFT, where a number of improvements (refinements) for the expression of the term A^{hs} was introduced. It can be summed up that the revisited PC-SAFT-based model seems to be robust for estimating the speed of sound in natural-gas systems. At this stage, predicting the sound speed in multicomponent mixtures seems quite encouraging for further research.

CONCLUSIONS

It was found that the results obtained in calculating the speed of sound in systems composed of oil and gas components are promising for the further use of the equation of state based on PC-SAFT for evaluating the thermodynamic properties of natural gas for practical purposes. No adjustable binary interaction parameters were used in this work, and the MAPE values in the sound speed for all binary and multicomponent mixtures studied were no more 2.5%, which is attributed to the strong physical basis of PC-SAFT-related models, including the examined version of this EOS. The CP-PC-SAFT EOS can be considered a suitable tool for the robust prediction of the speed of sound in various systems with reasonable accuracy for applications in chemical engineering.

ACKNOWLEDGMENTS

We thank I. Polishuk for his helpful comments and discussion.

This study was financially supported by a joint project of the Russian Foundation for Basic Research (RFBR) and the Iran National Science Foundation (INSF), INSF contract no. 96004167 and RFBR grant no. 17-58-560018.

SYMBOLS

A	Helmholtz energy, J
a, b	universal constants in CP-PC-SAFT model
C	heat capacity, J/(K mole)
d	distance between segments, Å
g	radial distribution function
I	abbreviated expression for the integral in perturbation theory

k	Boltzmann's constant or dimensionless fitting parameter
l	dimensionless fitting parameter
M_w	molecular mass, g/mole
m	number of segments per chain
N	number of experimental points
N_{av}	Avogadro number
P	pressure, Pa
R	gas constant
T	temperature, K
u	speed of sound, m/s
V	molar volume, m ³ /mole
x	molar fraction
δ	dimensionless parameter of volume displacement in CP-PC-SAFT
ϵ	depth of pair potential, J
ζ_k	abbreviated expression where $k = 0, 1, 2, 3, \text{Å}^{k-3}$
θ	dimensionless temperature
π	pi
ρ	molar density, mole/m ³
σ	segment diameter in CP-PC-SAFT, Å

INDICES

$0i, 1i, 2i$	numbers of universal constants in CP-PC-SAFT
av	Avogadro
c	critical state
$chain$	chain
$disp$	Dispersion
EOS	equation of state
hc	hard chain
hs	hard sphere
i, j	numbers of components or segments
L	liquid phase
n	total number of moles
P	isobaric conditions
res	residual contribution
T	isothermal conditions
tp	triple point
V	isochoric conditions
w	molecular mass
расч	calculated property
эксп	experimental property

REFERENCES

1. Meng, G., Jaworski, A.J., and White, N.M., Composition measurements of crude oil and process water emulsions using thick-film ultrasonic transducers, *Chem. Eng. Process.*, 2006, vol. 45, p. 383.

2. Machefer, S. and Schnitzlein, K., Inline concentration monitoring of binary liquid mixtures in the presence of a dispersed gas phase with a modified speed of sound immersion probe, *Chem. Eng. Technol.*, 2007, vol. 30, p. 1381.
3. de Medeiros, J.L., de Oliveira Arinelli, L., and de Queiroz F. Araújo, O., Speed of sound of multiphase and multi-reactive equilibrium streams: A numerical approach for natural gas applications, *J. Nat. Gas Sci. Eng.*, 2017, vol. 46, p. 222.
4. Nichita, D.V., Khalid, P., and Broseta, D., Calculation of isentropic compressibility and sound velocity in two-phase fluids, *Fluid Phase Equilib.*, 2010, vol. 291, p. 95.
5. Castier, M., Thermodynamic speed of sound in multiphase systems, *Fluid Phase Equilib.*, 2011, vol. 306, p. 204.
6. Farzaneh-Gord, M. and Rahbari, H.R., Numerical procedures for natural gas accurate thermodynamic properties calculation, *J. Eng. Thermophys.*, 2012, vol. 21, no. 4, pp. 213–234.
<https://doi.org/10.1134/S1810232812040017>
7. Farzaneh-Gord, M., Arabkoohsar, A., and Koury, R.N.N., Novel natural gas molecular weight calculator equation as a functional of only temperature, pressure and sound speed, *J. Nat. Gas Sci. Eng.*, 2016, vol. 30, pp. 195–204.
<https://doi.org/10.1016/j.jngse.2016.02.018>
8. Farzaneh-Gord, M., Mohseni-Gharyehsafa, B., Toikka, A., and Zvereva, I., Sensitivity of natural gas flow measurement to AGA8 or GERG2008 equation of state utilization, *J. Nat. Gas Sci. Eng.*, 2018, vol. 57, p. 305.
9. Llovel, F., Peters, C.J., and Vega, L.F., Second-order thermodynamic derivative properties of selected mixtures by the soft-SAFT equation of state, *Fluid Phase Equilib.*, 2006, vol. 248, p. 115.
10. de Villiers, A.J., Schwarz, C.E., Burger, A.J., and Kontogeorgis, G.M., Evaluation of the PC-SAFT, SAFT and CPA equations of state in predicting derivative properties of selected non-polar and hydrogen-bonding compounds, *Fluid Phase Equilib.*, 2013, vol. 338, p. 1.
11. Chapman, W.G., Gubbins, K.E., Jackson, G., and Radosz, M., New reference equation of state for associating liquids, *Ind. Eng. Chem. Res.*, 1990, vol. 29, p. 1709.
12. Huang, S.H. and Radosz, M., Equation of state for small, large, polydisperse, and associating molecules, *Ind. Eng. Chem. Res.*, 1990, vol. 29, p. 2284.
13. Huang, S.H. and Radosz, M., Equation of state for small, large, polydisperse, and associating molecules: Extension to fluid mixtures, *Ind. Eng. Chem. Res.*, 1991, vol. 30, p. 1994.
14. Gross, J. and Sadowski, G., Perturbed-chain SAFT: An equation of state based on a perturbation theory for chain molecules, *Ind. Eng. Chem. Res.*, 2001, vol. 40, p. 1244.
15. Barker, J.A. and Henderson, D., Perturbation theory and equation of state for fluids: The square-well potential, *J. Chem. Phys.*, 1967, vol. 47, p. 2856.
16. Polishuk, I., Lubarsky, H., and NguyenHuynh, D., Predicting phase behavior in aqueous systems without fitting binary parameters II: Gases and non-aromatic hydrocarbons, *AIChE J.*, 2017, vol. 63, p. 5064.
17. Polishuk, I., Standardized critical point-based numerical solution of statistical association fluid theory parameters: The perturbed chain-statistical association fluid theory equation of state revisited, *Ind. Eng. Chem. Res.*, 2014, vol. 53, p. 14127.
18. Polishuk, I., Katz, M., Levi, Y., and Lubarsky, H., Implementation of PC-SAFT and SAFT + Cubic for modeling thermodynamic properties of haloalkanes. I. 11 halomethanes, *Fluid Phase Equilib.*, 2012, vol. 316, p. 66.
19. Burgess, W.A., Tapriyal, D., Gamwo, I.K., Wu, Y., McHugh, M.A., and Enick, R.M., New group-contribution parameters for the calculation of PC-SAFT parameters for use at pressures to 276 MPa and temperatures to 533 K, *Ind. Eng. Chem. Res.*, 2014, vol. 53, p. 2520.
20. Lubarsky, H. and Polishuk, I., Implementation of the critical point-based revised PC-SAFT for modelling thermodynamic properties of aromatic and haloaromatic compounds, *J. Supercrit. Fluids*, 2015, vol. 97, p. 133.
21. Liang, X., Maribo-Mogensen, B., Thomsen, K., Yan, W., and Kontogeorgis, G.M., Approach to improve speed of sound calculation within PC-SAFT framework, *Ind. Eng. Chem. Res.*, 2012, vol. 51, p. 14903.
22. Palma, A.M., Queimada, A.J., and Coutinho, J.A.P., Using a volume shift in perturbed-chain statistical associating fluid theory to improve the description of speed of sound and other derivative properties, *Ind. Eng. Chem. Res.*, 2018, vol. 57, p. 11804.
23. Melent'ev, V.V., Postnikov, E.B., and Polishuk, I., Experimental determination and modeling thermophysical properties of 1-chlorononane in a wide range of conditions: Is it possible to predict a contribution of chlorine atom?, *Ind. Eng. Chem. Res.*, 2018, vol. 57, p. 5142.
24. Prikhod'ko, I.V., Samarov, A.A., and Toikka, A.M., On application of PC-SAFT model for estimating the speed of sound in synthetic and natural oil-and-gas mixtures, *Russ. J. Appl. Chem.*, 2019, vol. 92, no. 2, p. 262.
25. *NIST Chemistry WebBook*, NIST Standard Reference Database No. 69, Gaithersburg, Md.: National Institute of Standards and Technology (NIST), 2018.
<https://doi.org/10.18434/T4D303>
26. Ahmadi, P., Chapoy, A., and Tohidi, B., Density, speed of sound and derived thermodynamic properties of a synthetic natural gas, *J. Nat. Gas Sci. Eng.*, 2017, vol. 40, pp. 249–266.
<https://doi.org/10.1016/j.jngse.2017.02.009>
27. Younglove, B.A., Frederick, N.V., and McCarty, R.D., *Speed of Sound Data and Related Models for Mixtures of Natural Gas Constituents*, NIST Monograph, no. 178, Washington, DC: U.S. Government Printing Office, 1993.
28. Costa Gomes, M.F. and Trusler, J.P.M., The speed of sound in two methane-rich gas mixtures at temperatures between 250 K and 350 K and at pressures up to 20 MPa, *J. Chem. Thermodyn.*, 1998, vol. 30, p. 1121.